Design of a Bicycle Rig

By
Rastislav Racz

Submitted to the Department of Mechanical
Engineering in Partial Fulfillment of the Requirements for the Degree of

Bachelor of Science at the Massachusetts Institute of Technology
June 2010

ature of
Author.................................... ....
....
Department of Mechanical Engineering
May 7, 2010

Certified by
....
.....
Kim B. Blair
Researcher Engineer of Department of Aeronautics and Austronautics
Thesis Supervisor

Certified by
....
.....
Alexander H.Slocum
Neil and Jane Pappalardo Professor of Mechanical Engineering MacVicar Faculty Fellow
Thesis Supervisor

Accepted by
....
...
Professor J. Lienhard V
Collins Professor of Mechanical Engineering
Chairman, Undergraduate Thesis Committee

Design of a Bicycle Rig

by

Rastislav Racz

Submitted to the Department of Mechanical Engineering
On May 7th, 2010 in Partial Fulfillment of the
Requirements for the Degree Bachelor of Science in
Mechanical Engineering

Abstract

A design of a bicycle (bike) rig was conducted. This bike rig is designed to be used for aerodynamics measurement testing of bicycles, cyclists and cycling related items in a wind tunnel. This paper discusses the design of a new version of the bike rig that has been used in the MIT Wright Brothers Wind Tunnel. Through finite element analyses, feasibility and practicality studies the best bike rig was designed. A three groove kinematics coupling principle was used in the design of the measurement device of the rig. This paper contains detailed description of the working principle of the bike rig. This paper can also serve as instructions for building a new bike rig.

Thesis Supervisor: Kim B. Blair
Title: Researcher Engineer of Department of Aeronautics and Austronautics

Thesis Suprvisor: Alexander H. Slocum
Title: Neil and Jane Pappalardo Professor of Mechanical Engineering, MacVicar Faculty Fellow

Acknowledgements

I would like to acknowledge the contributions of several key people who made this project possible: Prof. Alexander Slocum of the Department of Engineering, for helping me solve countless number of issues and difficult problems throughout the project; Dr. Kim Blair of the Department of Aeronautics and Astronautics for advising throughout the project and Zach Labry MIT graduate student for acting as a resource and help.

Table of Contents

Page

List of Figures

List of Appendices

---

[1] Bicycle Trainer Data Logging and Control System Design, MIT, Wright Brother Wind Tunnel, Herman Chee, May 31, 2007

[2] Massachusetts Institute of Technology, Wright Brother Wind Tunnel, Information for use by Industry

[3] http://www.google.com/imgres?imgurl=http://www.mech.utah.edu/~me4000/tutorials/introProMechanica/images/sixDegreesOfFreedom.jpg&imgrefurl=http://www.mech.utah.edu/~me4000/tutorials/introProMechanica/constraints.html&h=307&w=586&sz=30&tbnid=uS_IOgqAgHz66M:&tbnh=71&tbnw=135&prev=/images%3Fq%3Dsix%2Bdegrees%2Bof%2Bfreedom&usg=__S837OA8kFeSVWvu_u0TyrfLiJp8=&ei=dpbTS7aPA4GBlAeVxYntDA&sa=X&oi=image_result&resnum=5&ct=image&ved=0CBkQ9QEwBA

Introduction

The objective of this thesis project is to design a bike rig- a device that supports a bike and enables measurements of drag and side forces exerted on a bike and a cyclist when the rig is used in a wind tunnel. Tests of aerodynamics of bikes, helmets, body positions and other cycling related elements have been conducted at the M.I.T. Wright Brothers Wind Tunnel (WBWT) under the supervision of Dr. Kim Blair. During these tests, the WBWT 6-axis load cell and a bike rig have been used.

This paper describes the part of the rig containing the measurement device. After implementing the remaining parts of the rig (rollers, motors, etc.) the whole assembly will improve the way tests are conducted by enabling acquisition of more accurate data and simplifying the process of putting a bike on a rig which is currently somewhat cumbersome. The more accurate data acquisition will be acquired through elimination of temperature drift and the ease of use will be improved by a better design. On top of that, one will be able to use this rig in different wind tunnels which will enable comparison of test data of one bike in different testing facilities. There are several ways to measure drag and side force on a bike rig. The most substantial part of this project is to find the best measurement device (most accurate, most reliable) and to design the bike rig containing this measurement device.

Requirements

The key data that will be measurable by the new rig are drag, yaw angle, power output, speed and temperature. Temperature can be measured with a regular thermometer but it needs to be insured that temperature is included in the measurement data as change in temperature can influence the performance of the measurement device.

Current Design

The current bike rig consists of an aluminum structure of an X shape. The "extremities" serve for holding the bars that stabilize the wheels of the bike (Figures 1, 2). The "body" of the rig contains rollers and is adjustable for different sizes of bikes. The adjusting is made manually and is rather complicated and imprecise. In the current rig, the adjusting mechanism consists of two concentric beams within each other. One can pull out or push in the inner beam, however, there is a lot of friction in this process and one cannot move the beams smoothly. All adjustments are made by sudden shocks which help to move the beams. This process is imprecise because there is no scale or grid and the only way of telling the size is by eye. Also the process does not consist of smooth transitions but rather sudden leaps. This process is cumbersome and impractical which is the main reason behind the design of a new rig.

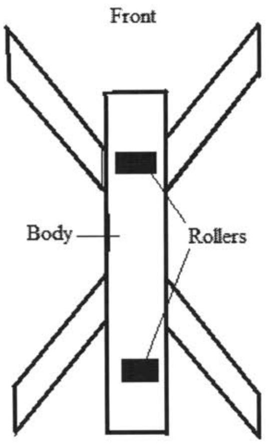

Figure 1, Top view of the current bike rig

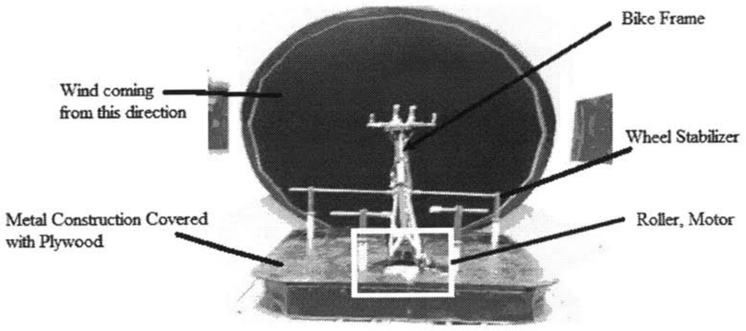

Figure 2, Current Bike Rig setup for testing in WBWT[4]

The wheel stabilizers are metal rods that slide into a hollow cylinder. These rods can be manually moved up and down to adjust for the wheel size. It requires the same adjusting mechanism as the body and is therefore imprecise. There is a threaded rod running perpendicularly through each of these rods. These threaded rods can be tightened manually which constraints the motion of the wheel and assures the stability. The tightening process is especially cumbersome and not very precise. Once the rig is assembled all opening and holes are covered with plywood and plastic material to ensure good aerodynamic conditions for testing. The rig is connected to the 6 axis load cell of the WBWT through the floor (Figure 3).

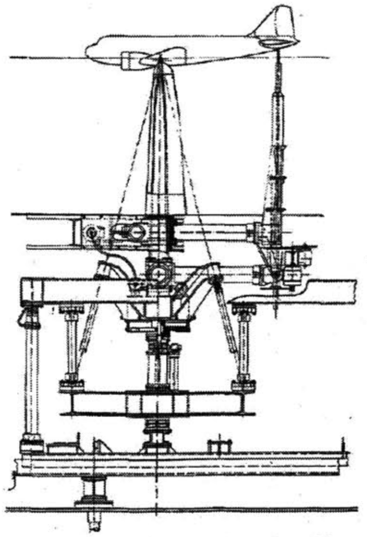

Figure 3, Side view of the 6 axis load cell inside the WBWT[4]

---

[4] Massachusetts Institute of Technology, Wright Brother Wind Tunnel, Information for use by Industry

New Design

Selection Process

This part consists of two subparts. At first, the paper approaches the steps that were taken during the design. These steps can be used during the fabrication of the bike rig and for its future improvement. The second part specifies the measurement device that the new bike rig will have.

In order to design a good bike rig several brainstorming sessions were organized in which Dr. Kim Blair, Zach Labry (MIT Graduate student) and I, each came up with many ideas. We then selected the best ideas and compared them to each other and to our idea of a theoretical ideal design. Several discussions in which we compared pros and cons of each design took place. In the end we made a ranking of top 19 ideas based on a scoring matrix which contained a set of criteria. Each design received a certain number of points from 1 to 10 for each criterion. The design with the highest number of points was chosen as the best design for the bike rig. See Figure 4 for more details.

Item number	10- best 1- worst Name	Takes measurements/ holding mechanism?	Easilly transported?	Safe and stable	Low Aerodynamic Interference	How much change to the current wind tunnel?	The Ease of mounting the rig on this system	Reliability (how much would friction or environment influence our data)	Ease of calibration	Reliability of calibration (sensitivity to environment)?	Access to Strain Gauges. Do they exist at all?	Total
1	**Flexuers and Loadcell**	measures, holds	5	10	5	10	5	10	5	10	10	60
2	**Embedded base with 8 strain gages**	measures, holds	5	10	5	10	5	10	5	10	10	60
3	**Stacked stage**	measures, holds	5	10	5	10	5	10	5	10	10	60
4	**Bed of nails**	measures, holds	1	2	3	8	5	2	2	5	5	28
5	**Orthogonal tubes**	holds	5	5	5	10	5	8	5	10	NA	53
6	**Vacuum preloaded air bearing**	holds	5	10	5	10	5	10	10	10	?	65
7	**The boat**	measures	10	NA	5	5	10	0	5	0	10	35
8	**Pneumatic balance**	measures, holds	5	10	5	10	5	10	5	10	10	60
9	**Commercial 2 axes load cell**										?	0
10	**Robot**	measures	10	NA	2	10	5	1	5	1	8	34
11	**Calibrated damper**	measures, holds	2	10	5	8	5	10	5	10	10	55
12	**Existing balance**	measures, holds	1	10	10	10	10	10	5	1		57
13	**Fish (spring) scale**	measures	10	NA	5	5	10	0	5	0	10	35
14	**Flexure with strain gauge**	measures, holds	5	10	5	10	5	10	5	10	10	60
15	**Roller skate**	holds	10	3	5	10	10	5	5	10	NA	58
16	**2 Axis roller with strain gauge**	holds	10	10	5	10	10	7	5	10	NA	67
17	**Magnetic Fiekd**	measures	?	?	10	10	10	10	5	10	1	55
18	**Tail Fin**										?	0
19	**Annular air bearing**	holds	10	10	7	10	3	5	5	10	NA	60

Figure 4, Different rig designs and criteria

The "Flexures and Load cell" bike rig was chosen as the best design (Figure 5). Later, it was discovered that this rig would not be built because its measurement device is not perfect. The detail working mechanism and description are included, because they may serve as an inspiration for further improvements of the third generation of the bike rig. On top of that, most of the design can and should be used with a new measurement device.

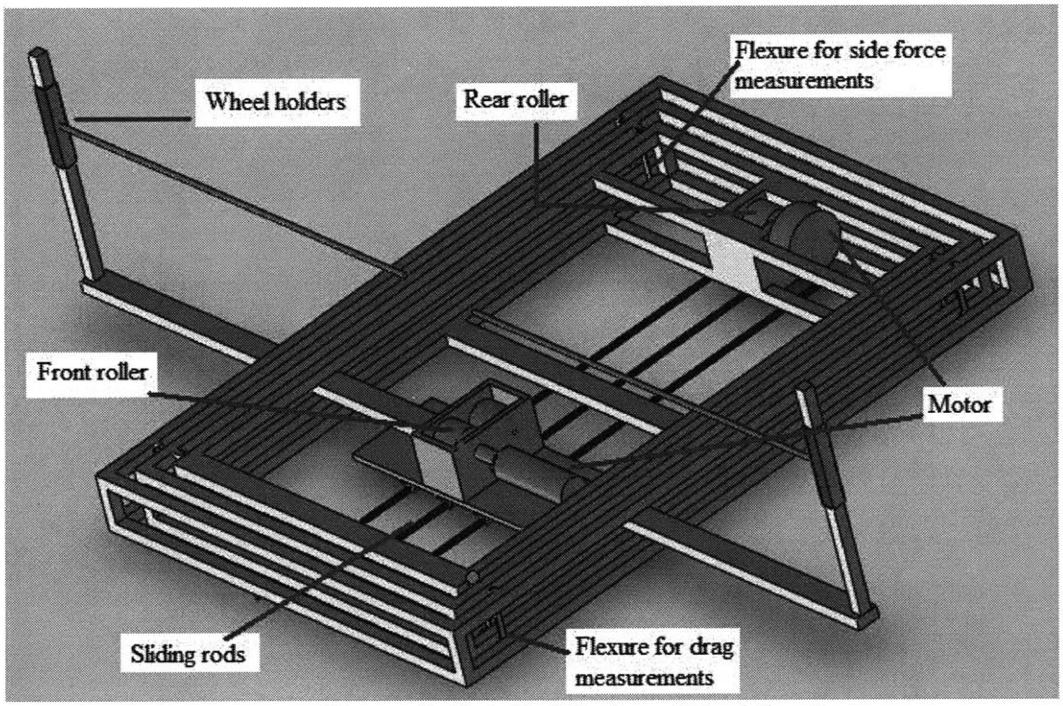

Figure 5, Detailed design of the bike rig

The design of the Flexures and Load Cell bike rig consists primarily of three concentric frames which are interconnected by flexures. These flexures contain strain gages and the output of the strain gauges provides the drag and side force exerted on the bike by the wind (Figure 6).

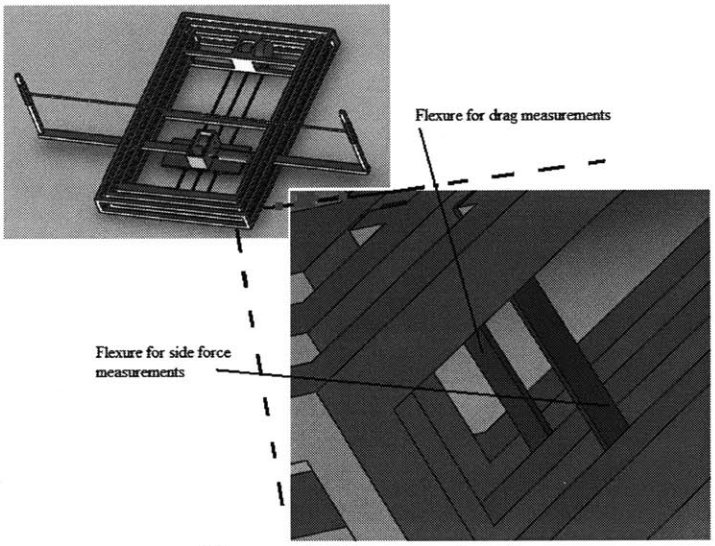

Figure 6, Flexures detail

Two sets of wheel holders (only front part shown in Figure 5) are used to keep the bike in a vertical position. These holders are metal rods that fit into the skewer orifice in a wheel's hub. They serve as clamps that clamp on the wheel from both sides and support the bike laterally. This prevents the bike from tilting to the side and it also provides rigidity when a cyclist pedals during testing. The mechanism is similar to the current rig's one, however, the new rig will have a pull out/ push in knob on the side of the vertical bars (similar to knobs that are used to fix weights during weight lifting). The vertical bars will be marked to ensure exact vertical position of the wheel holder beam. As a result this will improve the ease of use and precision of experiments.

Three sliding rods are used to move the front roller to adjust for different sizes of bikes (Figure 7). The lateral rods serve as supports and run through bearings that are attached to the outmost frame. The middle rod is smaller in diameter, which make it carry less load than the two lateral rods and is threaded. Using a crank, the middle rod will be used to precisely modify the size of the rig for different bikes. It will contain a gauge

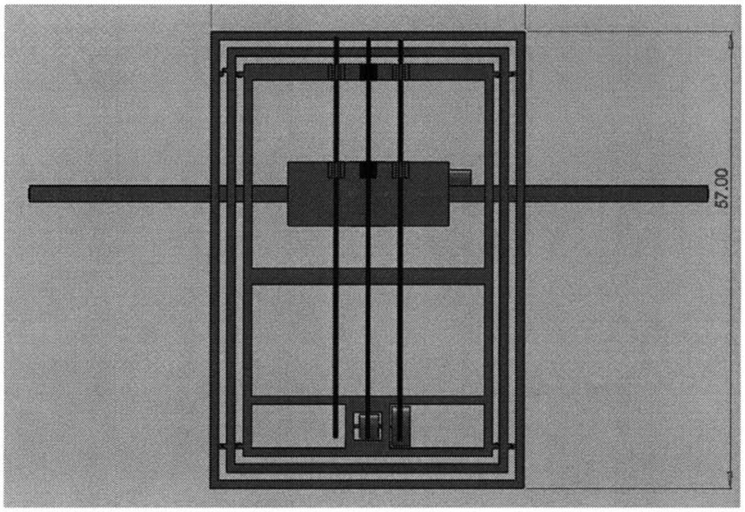

Figure 7, Bottom view of the rig- Sliding rods

When the cyclist starts pedaling, the rear wheel starts rotating, which powers a dynamo, which in turn power the front wheel. See Figure 8 for design details. By ensuring that both wheels spin we will get more representative data of real life conditions. When everything is ready for testing, all the void openings will be covered to provide good aerodynamic testing conditions. The rig will be lightweight which will make it easy to pick up and move to other location.

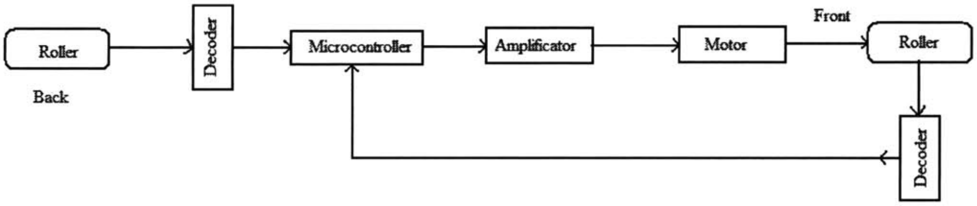

Figure 8, Electromechanical system powering the front wheel

The “Flexure and Load Cell” design fails in its measuring device mechanism. We deal with 6 degrees of freedom (DOF); force in x, y, z- direction and rotation around x, y, z- axis (see Fig. 8), however, we have 8 constraints (8 flexures). It becomes a problem of solving 6 equations of 8 unknown.

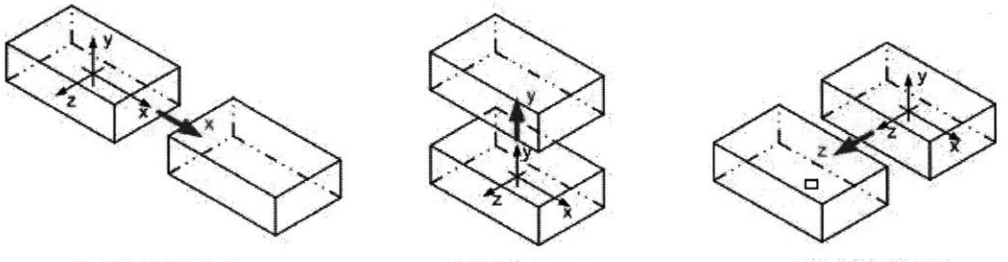

Linear in x-direction Linear in y-direction Linear in z-direction

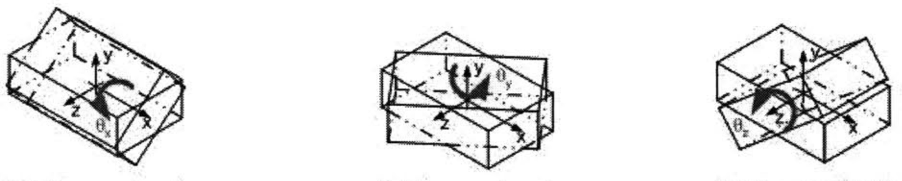

Rotation around x-axis Rotation around y-axis Rotation around z-axis

Fiure. 9, Representation of six degrees of freedom present in the bike rig system[5]

We could lower the number of flexures to 6 or, in order to conserve symmetry, even to 4. Having only 4 flexures would mean that each one of them would have to support more load. In order to support more load their geometry would have to change and this changed geometry would not enable us to measure strains because they would be of the order of 10^{-5} and less which are not measurable by strain gauges.

As a result a new measurement device needed to be found. The “Flexure and Load Cell” bike rig can be used as the “body” or “structure” for the new bike rig, onto which the correct measurement device needs to be built.

Measurement Device

The main idea behind using three groves kinematic coupling system in any design is to obtain statically determinate structure. We will constrain the 6 DOG system using exactly 6 constraints. This would make the system solvable and we could calculate for drag and side force, which are of our primary interest.

---

[5] http://www.google.com/imgres?imgurl=http://www.mech.utah.edu/~me4000/tutorials/introProMechanica/images/sixDegreesOfFreedom.jpg&imgrefurl=http://www.mech.utah.edu/~me4000/tutorials/introProMechanica/constraints.html&h=307&w=586&sz=30&tbnid=uS_IOgqAgHz66M:&tbnh=71&tbnw=135&prev=/images%3Fq%3Dsix%2Bdegrees%2Bof%2Bfreedom&usg=__S837OA8kFeSVWvu_u0TyrfLiJp8=&ei=dpbTS7aPA4GBlAeVxYntDA&sa=X&oi=image_result&resnum=5&ct=image&ved=0CBkQ9QEwBA

A simple understanding of the working principle of three grooved kinematic coupling can be done by looking at figures 10 and 11, which are the work of Prof. Alexander H. Slocum[6]. If we put three balls into three grooves that are part of a platform (the balls and the grooves need to be of specific dimensions) in such a way that they touch the walls of the grooves in one point only, and cover it with a flat platform, we can constraint 3 DOF. Now imagine the balls are actually half balls and are part of the top platform. After joining the 2 platforms, we will not be able to move the two platforms in respect to each other (other than separating them in the z-direction) in any way. Putting sensors on the contact points of the balls with the walls of the grooves will enable us to calculate the forces that act on the system. Figure 10, the traditional model, shows the two platforms joint while figure 11 shows the grooved platform with the balls. For more information, see footnotes 5 and 5 which refer to the work of Alexander H. Slocum or Slocum, A.H., "Design of Three-Groove Kinematic Couplings", *Precision Engineering*, Vo. 14, No. 2, pp 67-76.

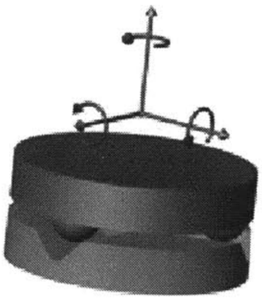
[7]

Figure 10, Traditional coupling diagram

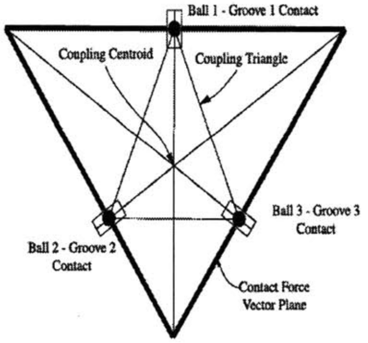

[8]

Figure 11, Model triangular layout

---

[6] http://pergatory.mit.edu/kinematiccouplings/

[7] Slocum, A.H., "Design of Three-Groove Kinematic Couplings", Precision Engineering, Vo. 14, No. 2, pp 67-76

8 Slocum, A.H., "Design of Three-Groove Kinematic Couplings", Precision Engineering, Vo. 14, No. 2, pp 67-76

In our system, we are not using grooves but we simulate the same working mechanism by using V-brackets, and air bearings. See figure 12. The 90° V-brackets play the role of the groove and provide a one point contact with the rest of the system. There are two V-brackets which contain a load cell and an air bearing between them. The load cell is attached to the top V-bracket and is connected with the air bearing through a ball-one point contact. The purpose of the air bearing is the elimination of friction and hence assuring that the double V- bracket system is a one point contact system.

The three V-bracket systems are set up in such a way that the two V-brackets, that are on the rear side of the rig are equidistant from the third one and are axially symmetrical to each other (Figure 12-16). This ensures the stability of the system and the possibility of creating a statically determinate structure. For maximal stability, the axis of the three V-Brackets intersects in the point which is the center of the circle containing these three V-Brackets. The position of the load cells makes it possible to avoid the influence of temperature on the data. The temperature will affect all load cells in the same way and since the load cells are paired up one and one in opposite directions, the difference due to temperature will cancel out. For example if one load cell measures a higher load in the x-direction, the load cell facing the opposite direction will measure a higher load in the –x- direction and the difference will cancel out.

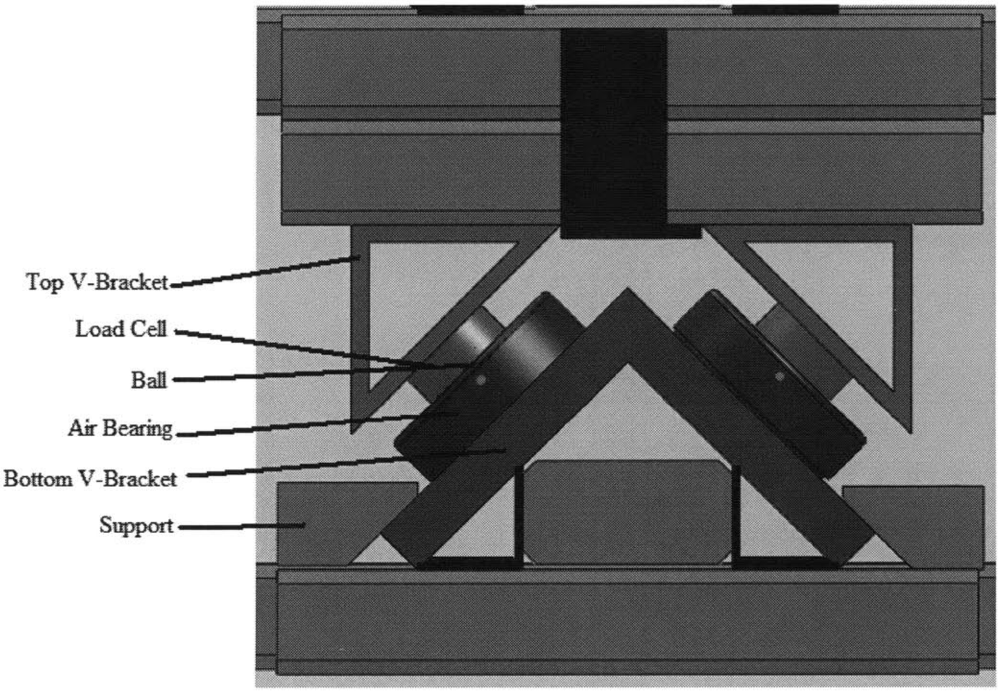

Figure 12, Detail of the V-bracket mechanism

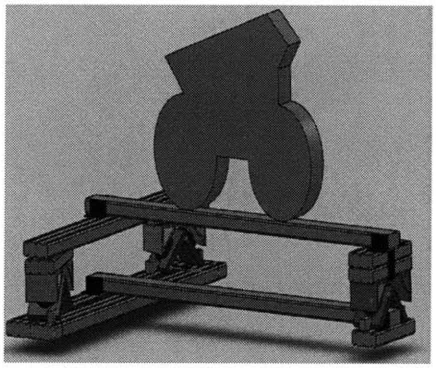
Figure 13, Bike Rig with a Bike

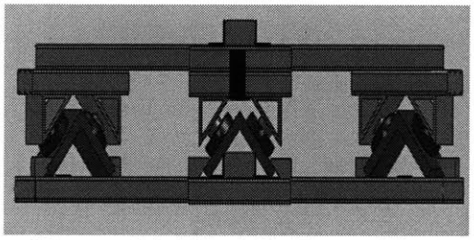
Figure 14, Bike Rig Front View

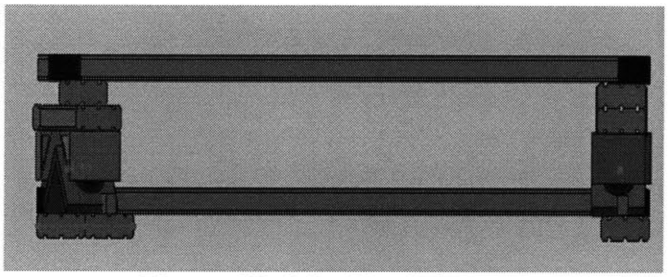
Figure 15, Bike Rig Side View

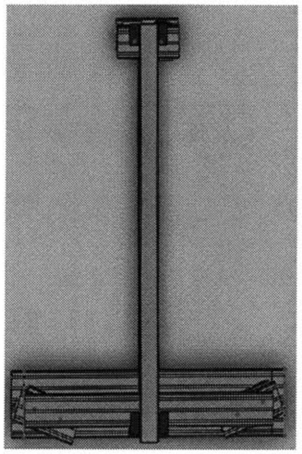
Figure 16, Rig Top View

Force Calculation

We can model the system consisting of the bike in the wind tunnel using a free body diagram (FBD), see figure 17.

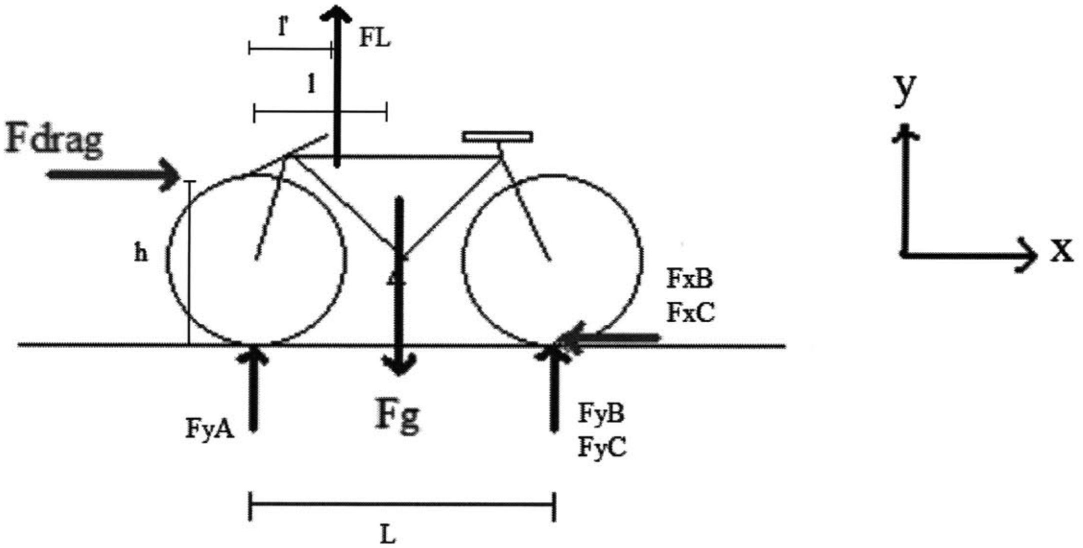

Figure 17, Freed body diagram of the bike rig with the bike in a wind tunnel

$$\sum F_x = F_D + F_{xB} + F_{xC} \qquad (1)$$

$$\sum F_y = -F_g + \sum F_y + F_L \qquad (2)$$

$$\sum F_z = F_{zA} + F_{zB} + F_{zC} \qquad (3)$$

$$\sum T_A = -F_D \times h + \sum F_y \times L - F_g \times l + F_L \times l' \qquad (4)$$

The force of the wind acting on the bike is a force field that is modeled as a vector F_{Drag} acting on the system (bike + rider) at a height h from the surface of the rig. There are three V-bracket systems each containing two load cells. The output that we receive from each load cell is represented as vector perpendicular to the surface of the V-bracket (Figure 16).

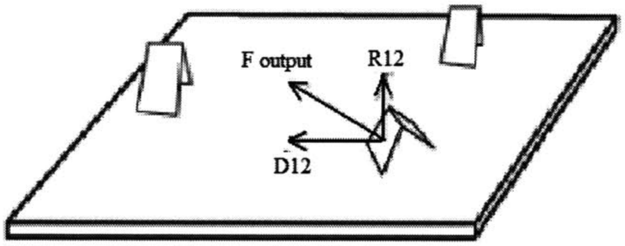

Figure 18, Vector Model of the Output of a Load Cell

The x-components of each load cell vector is called F_{xi} the subscripts specify the load cell) and the y-component of each load cell vector is called F_{yi} (with similar subscript specifications) (Fig. 18). F_L is the lift force that acts on the system.

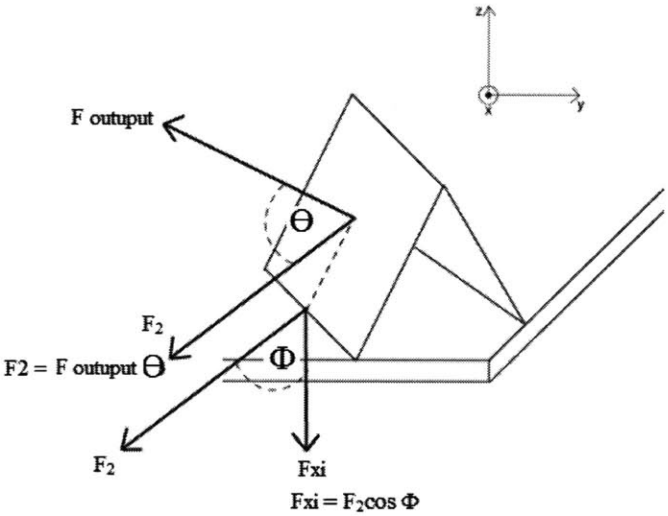

Figure 19, Vector Decomposition of the Output of a Load Cell

$$F_2 = F_{output} \times \cos\theta \tag{5}$$

$$F_{xi} = F_2 \times \cos\phi \tag{6}$$

$$F_{xi} = F_{output} \times \cos\theta \times \cos\phi \tag{7}$$

The output information will be represented as a magnitude of the vector, but knowing the dimensions of the V-brackets and their position on the platform, allows us use trigonometry to calculate the x, y and z- components of this vector (equations 5-6). Because of the position of the front V-bracket (Fig 13) there are no x-components on this V-bracket, however there is a y-component on each V-bracket. Using equations 1-4, the magnitude of the drag force F_{Drag} can be determined.

There are six load cells in the system and therefore we will receive six outputs. Each load cell's output can be decomposed into x, y and z- direction. After this decomposition, all the x, y and z-components will be added to form the F_x, F_y and F_z forces respectively.

For the V-Bracket in the front of the rig (called A) the calculation of the vector forces components for each load cell (called 1 and 2):

$$F_x = 0 \tag{8}$$

$$F_y = F_{A1} \times \sin\theta \tag{9}$$

$$F_z = -F_{A1} \times \cos\theta \tag{10}$$

$$F_x = 0 \tag{11}$$

$$F_y = F_{A2} \times \sin\theta \tag{12}$$

$$F_z = F_{A2} \times \cos\theta \tag{13}$$

Resultant forces from load cells on V-Bracket A:

$$F_{xA} = 0 \tag{14}$$

$$F_{yA} = (F_{A2} + F_{A1}) \times \sin\theta \tag{15}$$

$$F_{zA} = F_{A2} - F_{A1} \times \cos\theta \tag{16}$$

Similarly, we can calculate the magnitudes of the x, y and z- components of the output vector of the two other V-brackets B and C. Each bracket contains 2 load cells called 1, 2.

Load Cell B

$$F_{xB} = (F_{B2} - F_{B1}) \times \cos\theta \times \cos\phi \tag{17}$$

$$F_{yB} = (F_{B2} + F_{B1}) \times \sin\theta \tag{18}$$

$$F_{zB} = F_{B2} - F_{B1} \times \cos\theta \tag{19}$$

Load Cell C

$$F_{xC} = (F_{C2} - F_{C1}) \times \cos\theta \times \cos\phi \tag{20}$$

$$F_{yC} = (F_{C2} + F_{C1}) \times \sin\theta \tag{21}$$

$$F_{zC} = F_{C1} - F_{C2} \times \cos\theta \tag{22}$$

The final calculation of the forces Fx, Fy and Fz acting on the rig is the sum of all the forces in each direction.

$$F_x = F_{xA} + F_{xB} + F_{xC} = 0 + (F_{B2} - F_{B1}) \times \cos\theta \times \cos\phi + (F_{C2} - F_{C1}) \times \cos\theta \times \cos\phi \tag{23}$$

$$F_{yC} = (F_{C2} + F_{C1}) \times \sin\theta = (F_{A2} + F_{A1}) \times \sin\theta + (F_{B2} + F_{B1}) \times \sin\theta + (F_{C2} + F_{C1}) \times \sin\theta \tag{24}$$

$$F_{zC} = F_{C1} - F_{C2} \times \cos\theta = F_{A2} - F_{A1} \times \cos\theta + F_{B2} - F_{B1} \times \cos\theta + F_{C1} - F_{C2} \times \cos\theta \tag{25}$$

Assembly

Most of the material used for the assembly of the rig is from 8020. This type of material was chosen for its ease of use and practicality. The rig consists primarily of three parts: Bottom platform, V-Brackets, Top platform.

The rear bottom platform is made of two 44'' x 4.5'' x 1.5'' beams connected together. The front bottom part consists of a single 10'' x 4.5'' x 1.5''beam. These beams carry the middle part, V-brackets. The brackets themselves are made of steel and are right angle blocks of dimensions 5'' long and of 5'' side length. The front bracket is parallel to the face of the base. The rear brackets are under 70.67° angle. This angle was determined in order to ensure the best stability of the system, based on the size of the triangle the V-Bracket forms. The axes of the angles meet at the center of the circle containing the V-brackets. The brackets are supported by aluminum pieces which hold it down. There is a 57'' long beam connecting the front with the back.

The air bearing sits on top of the bottom V-bracket and is connected to the load cell through a ball (the both have a little opening for the placement of the ball) of ¾'' diameter. The load cell is glued onto the bottom part of the top V-bracket. The load cell is a Futek load cell of maximum measurable load 100lbs and sensitivity 0.05lbs.
The top V-bracket is a pyramidal structure that is connected to a beam of dimensions 10'' x 4.5'' x 1.5''. There are three identical structures forming a triangle. The top part of the rig consists of beams which connect the V-brackets together.

A detailed list of material and the material order can be found in Appendix.

Conclusions and Recommendation

This paper managed to describe the design of a new bike rig for aerodynamics measurements of cycling related testing in a wind tunnel. It also contains the detailed instructions that are needed for building this rig. The main design is the 3 groove kinematics coupling design of the measurement device. It can be used instead of the load cell currently used for this kind testing in the MIT WBWT.

This paper does not provide a detailed description of the entire bike rig design but focuses on the measurement device. However, it is recommended to study the material specifying the design process in this paper, when making the holistic design of a bike rig containing the measurement device, rollers, motors and other hardware parts.

Appendix

Material Order

	Part	Material	Size	Quantity	Price	Total
Bottom Side	Rear Platfrom	**8020 (1545)**	44in	2	$1.40/in	$ 123.20
	Front Platform	**8020 (1545)**	10in	1	$1.40/in	$ 14.00
	Rear to Front Beam	**8020 (1530)**	57in	1	$0.93/in	$ 53.01
Top Side	Rear Platform	**8020 (1545)**	40in	1	$1.40/in	$ 56.00
	Spacer Platform	**8020 (1545)**	10in	4	$1.40/in	$ 56.00
	Rear to Front Beam	**8020 (1530)**	57in	1	$0.93/in	$ 53.01
V-Brackets	Pyramids	**8020 (8636)**	5in	6	$1.45/in	$ 43.50
	Bottom Supporters	McMaster 89215K326	1 x 1.24 x 12	1	$ 34.35	$ 34.35
Joints	L Joint	**8020 (4413)**	6 holes	8	$ 5.60	$ 44.80
	Flat Joint	**8020 (3280)**	8 holes	6	$ 5.95	$ 35.70
	Big Fat L Joint	**80280 (4016)**	6 holes	8	$ 6.60	$ 35.70
T-Nuts	For Joints	**8020 (3287)**	3 holes	16	$ 0.68	$ 10.88
		8020 (3280)	2 holes	24	$ 0.79	$ 18.96
	Pyramides	**8020 (3286)**	1 hole	12	$ 0.21	$ 2.52
	Bottom Supporters	**8021 (3286)**	1 holes	6	$ 0.21	$ 1.26
	Other					
Bolts	For Joints	**8019 (3065)**	1/4-20, 3/4	150	$ 0.27	$ 40.50
	Pyramides	**8020 (3065)**	1/4-20, 1.5	12	$ 0.27	$ 3.24
	Bottom Supporters	**8020 (3081)**	1/4-20, 2 1/8	6	$ 0.82	$ 4.92
	Other					
Total						**$631.55**